

PACS 42.79.Vb

Using ellipsometry methods for depth analyzing the optical disc data layer relief structures

V.G. Kravets¹, I.V. Gorbov²

*Institute for Information Recording, National Academy of Science of Ukraine
2, M. Shpaka str., 03113 Kyiv, Ukraine*

¹ Phone: (38-044) 454-21-19, fax: (38-044) 241-72-33, e-mail: vasyk_kravets@yahoo.com

² Phone: (38-044) 454-22-09, fax: (38-044) 241-72-33, e-mail: ivan-gorbov@list.ru

Abstract. We studied the relief depth of the data layer formed in a glass disk by ion beam etching process with using classical ellipsometry at the constant wavelength 632.8 nm for different angles of incidence. It was found that for 0° and 90° azimuth angles, a pair of ellipsometric parameters Ψ and Δ is sufficient to characterize the changes in light reflection for various structure depths. The depth of optical disc data layer relief structures was estimated via experimental dependences of ellipsometric parameters. The estimated data layer depths were found to be in good agreement with independent tunnelling electron microscopy measurements.

Keywords: data layer, optical disc, relief depth, ellipsometry, scatterometry, effective medium theory, effective refractive indices.

Manuscript received 13.12.07; accepted for publication 07.02.08; published online 31.03.08.

1. Introduction

Scatterometry is an attractive metrological technique for determining the grating parameters, such as the line-width and thickness from optical measurements. Previous researches have demonstrated the use of reflection scatterometry for characterizing 100 to 400 nm grating lines with a 100 to 500 nm pitch (or depth) [1, 2]. These characteristics were determined within a computational resolution of 10 nm. Classical scatterometry is limited to reflectance measurements for two configurations, in which the azimuth angle ϕ between the plane of incidence and the grating vector is 0° or 90°. In this work, we extended this method by performing ellipsometry-type measurements of a surface relief structure. This technique involves extracting the phase in addition to the measured amplitude of a reflected laser beam. For 0° or 90° azimuth angles, a pair of ellipsometric parameters Ψ and Δ is sufficient to characterize the reflection. A grating or compact-disc relief structure should be considered as anisotropic media due to their anisotropic geometry [3–5]. To describe this anisotropic media, we have employed the effective medium theory (EMT) [6, 7]. Within the scope of this theory, the relief structure is approximated as anisotropic medium that have effective refractive indices. Although the grating diffraction is rigorously

described by RCWA for rapid analysis of the relief structure in a technological process, the EMT is more convenient. In this work, we have used the second order EMT to estimate geometrical parameters of the CD-disc relief structure.

2. Theory

By using ion beam etching, the grating structures on the surface of glass were fabricated with various depth thicknesses. Fig. 1 displays the dependence of the surface profile depth for ion etched glass disc. Used for optical media data coding (EFM for CD, EFM+ for DVD, ETM for HD-DVD and 17PP for Blu-Ray) provides presence of 50 % pits and 50 % lands on every tracks. Then disc relief structure can be presented by the 1_D binary profile, which is illustrated in Fig. 2. It is assumed that grating profile is square, the geometry is completely defined by the depth thickness d , periodicity Λ , and profile width b . The period Λ was not considered as a fitting parameter, because the period value is very accurate with laser-beam lithography. Moreover, we could experimentally check the period accuracy with both AFM measurements and angular positions of higher diffraction orders at normal incidence of light. The hole walls of recorded bits were assumed to be perfectly vertical, and their shape was approximated by rounded

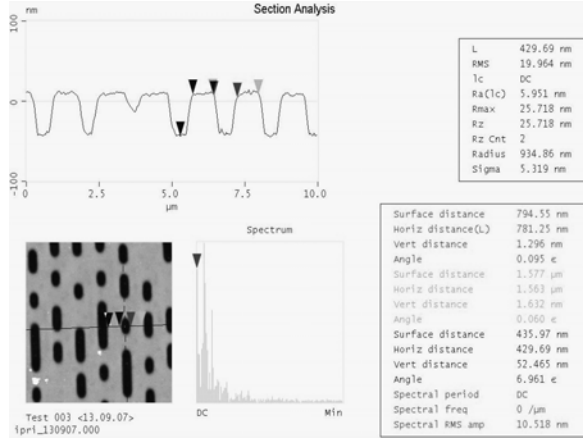


Fig. 1. The structure of data layer on the glass substrate surface.

squares. Any surface roughness of the glass substrate was neglected. The refractive index of the glass was taken from experimental values determined by spectroscopic ellipsometry. Finally, the depth and width of the holes were the only two adjustable parameters in the simulations used to fit the ellipsometric data. This structure (Fig. 2) can be treated as effective medium sandwiched between two homogeneous dielectrics. The second-order EMT theory is employed to analyze the disc structure. The medium of light incidence is air ($n_i = 1$), the filling factor f of the profile is equal to the ratio b/Λ , and the profile depth is d .

We will analyze only the zeroth order of scattered light to calculate the ellipsometric parameters: phase shift Δ and restored angle Ψ . It was shown in literature that the gratings of dielectric material act as homogeneous birefringent materials. In this case, there exists a difference between effective indices of refraction n_p for light polarized in the plane parallel to the grating and n_s – perpendicular to the layers of gratings.

The interaction of light with grating is accurately described by the rigorous coupled-wave analysis (RCWA) developed by Moharam and Gaylord [2-5]. According to this model, nanostructured surface of the disc is represented by an uniaxial anisotropic layer described by the effective parameters. In the second-order in the period-to-wavelength ratio Λ/λ , we can represent the effective dielectric function of the top layer in Fig. 2b that can be expressed as in [6, 7]:

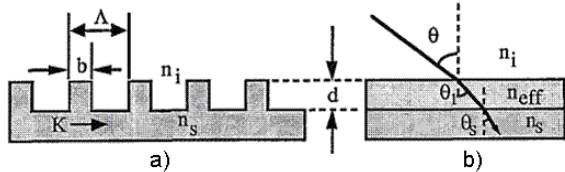


Fig. 2. The disc relief structure profile (a) and its view as effective medium sandwiched between two homogeneous dielectrics (b).

$$\varepsilon_{\text{eff}}^p = \varepsilon_{\text{eff}}^p(0) \times \left[1 + \frac{\pi^2}{3\beta^2} f^2 (1-f)^2 (n_s - n_i)^2 \varepsilon_{\text{eff}}^s(0) \left(\frac{\varepsilon_{\text{eff}}^p}{\varepsilon_i \varepsilon_s} \right)^2 \right], \quad (1)$$

$$\varepsilon_{\text{eff}}^s = \varepsilon_{\text{eff}}^s(0) \left[1 + \frac{\pi^2}{3\beta^2} f^2 (1-f)^2 \frac{(n_s - n_i)^2}{\varepsilon_{\text{eff}}^s(0)} \right], \quad (2)$$

where the filling factor f is given by

$$f = \frac{b}{\Lambda}. \quad (3)$$

The design constant β describes how much smaller the ratio Λ/λ is relatively to the ratio $1/(n_i + n_s)$.

$$\beta = \frac{\lambda}{\Lambda(n_i + n_s)}, \quad (4)$$

where $n_i = 1$ is the refractive index of air, and $n_s = 1.5$ is the refractive index of glass, while $\varepsilon_i = n_i^2$ and $\varepsilon_s = n_s^2$.

The effective dielectric function for the zeroth order is given by [6, 7]:

$$\frac{1}{\varepsilon_{\text{eff}}^p(0)} = \frac{f}{\varepsilon_s} + \frac{1-f}{\varepsilon_i}, \quad (5)$$

$$\varepsilon_{\text{eff}}^p(0) = f \varepsilon_s + (1-f) \varepsilon_i. \quad (6)$$

Using these parameters and formulas (1)-(6), we can calculate n_{eff} , which is represented at Fig. 2b for two polarizations of reflected light:

$$\left. \begin{aligned} n_{\text{eff}}^p &= (\varepsilon_{\text{eff}}^p)^{1/2} \\ n_{\text{eff}}^s &= (\varepsilon_{\text{eff}}^s)^{1/2} \end{aligned} \right\}. \quad (7)$$

After this procedure, we have all the refractive indexes (Fig. 2b) to calculate the Fresnel reflection coefficients.

$$r_{01}^p = \frac{(n_{\text{eff}}^p/n_i)^2 \cos \theta - [(n_{\text{eff}}^p/n_i)^2 - \sin^2 \theta]^{1/2}}{(n_{\text{eff}}^p/n_i)^2 \cos \theta + [(n_{\text{eff}}^p/n_i)^2 - \sin^2 \theta]^{1/2}}, \quad (8)$$

$$r_{01}^s = \frac{\cos \theta - [(n_{\text{eff}}^s/n_i)^2 - \sin^2 \theta]^{1/2}}{\cos \theta + [(n_{\text{eff}}^s/n_i)^2 - \sin^2 \theta]^{1/2}}, \quad (9)$$

$$r_{12}^p = \frac{(n_s/n_{\text{eff}}^p)^2 \cos \theta_1 - [(n_s/n_{\text{eff}}^p)^2 - \sin^2 \theta_1]^{1/2}}{(n_s/n_{\text{eff}}^p)^2 \cos \theta_1 + [(n_s/n_{\text{eff}}^p)^2 - \sin^2 \theta_1]^{1/2}}, \quad (10)$$

$$r_{12}^s = \frac{\cos \theta_1 - [(n_s/n_{\text{eff}}^s)^2 - \sin^2 \theta_1]^{1/2}}{\cos \theta_1 + [(n_s/n_{\text{eff}}^s)^2 - \sin^2 \theta_1]^{1/2}}, \quad (11)$$

where θ is the angle of incidence of the laser beam, and θ_1 is determined from the Snell law;

$$n_i \sin \theta = n_s \sin \theta_1,$$

where $n_i = 1$, $n_s = 1.5$.

We can write the equations for the total Fresnel reflection coefficients [9]:

$$r_p = \frac{r_{01}^p + r_{12}^p \exp(-i2\delta_p)}{1 + r_{01}^p r_{12}^p \exp(-i2\delta_p)}, \quad (12)$$

$$r_s = \frac{r_{01}^s + r_{12}^s \exp(-i2\delta_s)}{1 + r_{01}^s r_{12}^s \exp(-i2\delta_s)}, \quad (13)$$

where

$$\delta_p = 2\pi \left(\frac{d}{\lambda} \right) n_{\text{eff}}^p \cos \theta_1, \quad (14)$$

$$\delta_s = 2\pi \left(\frac{d}{\lambda} \right) n_{\text{eff}}^s \cos \theta_1, \quad (15)$$

where d is the grating thickness (Fig. 2).

If we have the Fresnel reflection coefficients r_p and r_s , we can write the main ellipsometry law [8]:

$$\frac{r_p}{r_s} = \tan(\Psi) \exp(i\Delta). \quad (16)$$

We carried out theoretical simulation for a CD-type disc structure to verify the diffraction sensitivity of the ellipsometric technique. Our parameters for calculation were as follows: $\Lambda = 1500$ nm, $b = 1500 - 600 = 900$ nm, $\lambda = 632.8$ nm, $n_i = 1$, $n_s = 1.5$. We performed the theoretical simulations of disc relief structures with the path line either parallel ($\phi = 0^\circ$, Ψ_0 , Δ_0) or normal ($\phi = 90^\circ$, Ψ_{90} , Δ_{90}) to the incident plane. Fig. 3 shows the Ψ_0 , Δ_0 variations versus the angle of incidence for various profile depths in glass. Second-order EMT predicts the minimum for the function of Ψ around Brewster angles. On the other hand, this theory predicts that the function of Δ must cross 90 deg. for these angles of incidence. As expected, both ellipsometric parameters Ψ_0 , Δ_0 are very sensitive to the depth d in the region of the Brewster angle of incidence for pure glass substrate ($\theta \approx 57^\circ$). These simulations were performed to characterize the changes in d of 10 nm. We can note that changes in the diffracted light parameters Ψ_0 and Δ_0 are sufficient to detect 10-nm variations in depth of the disc profile.

3. Experiment

The ellipsometric parameters Ψ_0 , Δ_0 and Ψ_{90} , Δ_{90} at $\lambda = 632.8$ nm of 7 disc profile structures were measured. He-Ne laser was used as the source of illumination. The incident beam passed through the polarizer and compensator and illuminated the disc structure. The glass disc was rotated about the vertical axis to provide ϕ variations. The ellipsometric parameters were measured for angles of incidence θ ranging from 50 to 65 degrees. This allowed us to determine the ellipsometric functions, as well as the minimum of the restored angle Ψ , which corresponds to the Brewster angle.

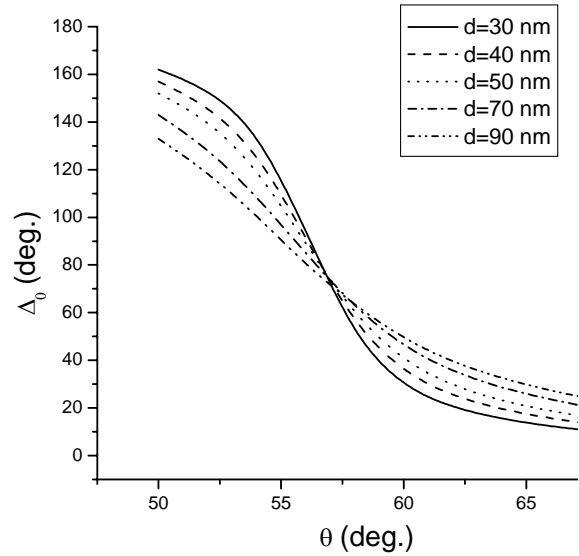
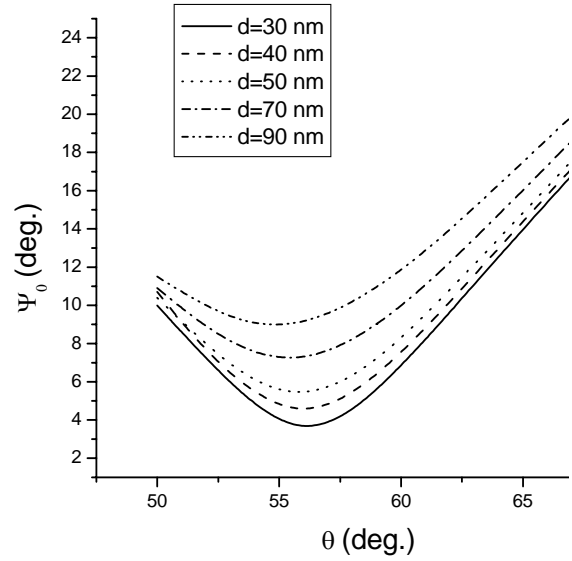


Fig. 3. The theoretical dependences of ellipsometrical parameters Ψ_0 , Δ_0 as a function of the angles of incidence for various profile depths of a glass CD disc.

Fig. 4 shows the experimental measurements of the functions Ψ_0 and Δ_0 for different values of the depth d . The experimental result shows the polarization effect from subwavelength profile features. Different depths, d , give different angle dependences of Ψ_0 and Δ_0 . The region in the vicinity of the Brewster angle $\theta_{\text{Br}} \approx 57^\circ$ can be used as sensitive signatures of the depth d .

Comparison of the experimental (Fig. 3) and theoretical (Fig. 4) curves gives that angle dependences of the ellipsometric parameters Ψ and Δ for different profile depth disc structures agree rather well with the second-order EMT calculations in predicting the thickness d for which the minimum of Ψ is reached and approximate homogeneous layer models provide a reasonable estimate of the thickness of the profile depth.

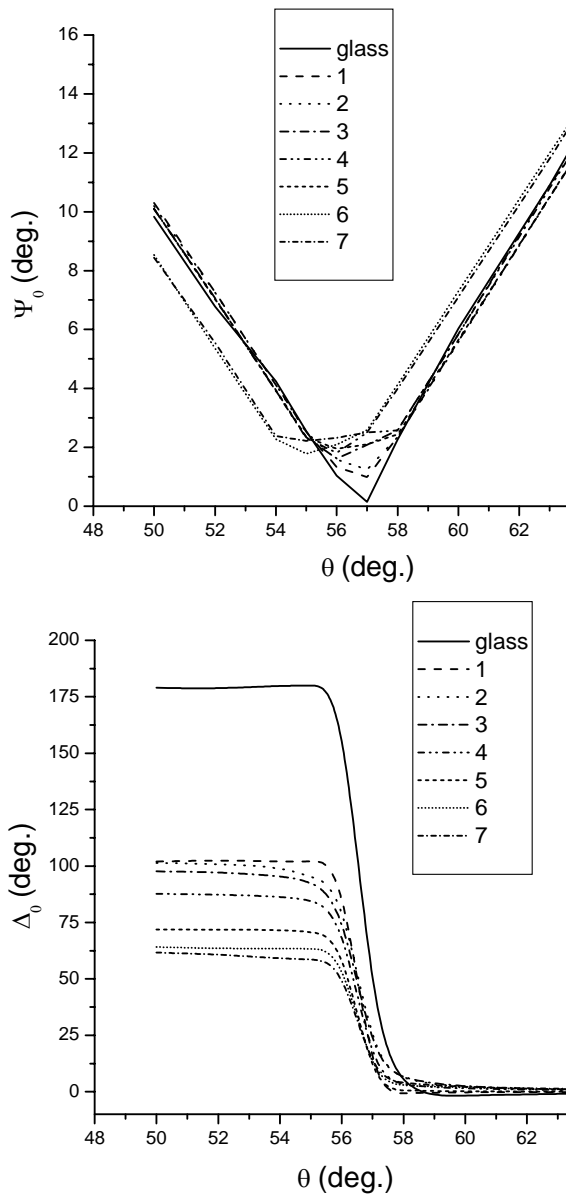


Fig. 4. The experimental dependences of ellipsometrical parameters Ψ_0 , Δ_0 as a function of the angles of incidence for various profile depths of a glass CD disc.

We performed measurements of disc relief structures with the path line either parallel ($\phi = 0^\circ$, Ψ_0 , Δ_0) or normal ($\phi = 90^\circ$, Ψ_{90} , Δ_{90}) to the plane of incidence. It is difficult to estimate the profile depth d directly from the data for Ψ and Δ , because it is difficult to determine values of minimums for functions Ψ and Δ . Then, to estimate the structure depth we have used diagrams $(\Delta_0 - \Delta_{90})$ versus the angle of incidence θ for various values of d (Fig. 5).

The dimensions of the disc profile were also measured before the optical measurements by atomic force microscopy. The agreement between these both measurements is reasonably good, although the value of d from optical measurements for small thicknesses is larger than the expected ones (Table).

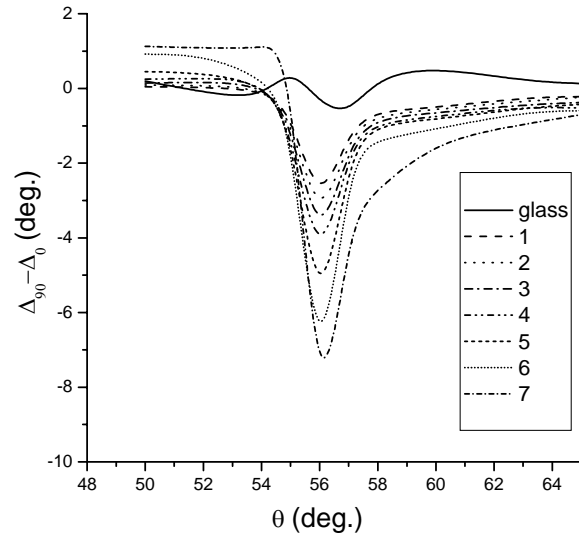


Fig. 5. Variations of $(\Delta_0 - \Delta_{90})$ versus the angle of incidence θ for different values of d for CD disc.

Table. Estimated value of the depth, d , for CD profiles in the case of width $b = 600$ nm.

Number of Test	Estimated depth, d (nm)	AFM, d (nm)
Test 120	30	30
Test 127	40	38
Test 130	45	45
Test V1	55	56
Test 155	70	75
Test 001	80	82
Test 011	90	93

4. Conclusion

We have demonstrated the feasibility of ellipsometric scatterometry for the metrology of the depth by analyzing the optical disc data layer relief structures within the accuracy of 5 nm. For correct reading optical discs by the standard player, the depth of relief structures must be 125 ± 30 nm, then the accuracy of proposed estimations is enough to control disc manufacture. Therewith, because material of substrate may consist of many components, the difference of even neighbour pit depth can reach 5 nm after ion beam etching. The diameter of scanning laser beam is about 3 mm, then almost 2000 data tracks get in the scanned area. It means that the averaged depth is estimated in contrast to analysis of a single pit by atomic-force microscope. Obtained results are extremely useful in the context of optical disc fabrication due to monitoring and controlling the depth of etching into a glass (dielectric) wafer in real time (in situ) by using ellipsometric measurements.

References

1. B.K. Minhas, S.A. Coulombe, S.Sohail, H. Naqvi, and J.R. McNeil, Ellipsometric scatterometry for the metrology of sub 0.1- μm -linewidth structures // *Applied Optics* **37**, p. 5112-5115 (1998).
2. X.-T. Huang and F.L. Terry, Spectroscopic ellipsometry and reflectometry from grating (scatterometry) for critical dimension measurement and in-situ, real-time process monitoring // *Thin Solid Films* **455-456**, p. 828-836 (2004).
3. M.G. Moharam and T.K. Gaylord, Diffraction analysis of dielectric surface-relief gratings // *J. Opt. Soc. Amer.* **10**, p. 1383-1392 (1982).
4. M.G. Moharam and T.K. Gaylord, Rigorous coupled-wave analysis of grating diffraction – E-mode polarization and losses // *J. Opt. Soc. Amer.* **73**, p. 451-455 (1983).
5. M.G. Moharam, E.B. Grann, and D.A. Pommet, Formulation for stable and efficient implementation of the rigorous coupled-wave analysis of binary gratings // *J. Opt. Soc. Amer. A* **12**, p. 1068-1076 (1995).
6. G. Campbell, Effective medium theory of sinusoidally modulated volume holograms // *J. Opt. Soc. Amer. A* **12**, p. 1113-1117 (1995).
7. Daniel H. Raguin and G. Michael Morris, Antireflection structured surfaces for the infrared spectral region // *Applied Optics* **32(7)**, p. 1155-1167 (1993).
8. M. Born and E. Wolf, *Principles of Optics*. Pergamon, Oxford, p. 708, 1985.